HHS Public Access
Author manuscript
Clin Image Based Proced. Author manuscript; available in PMC 2017 January 30.

Published in final edited form as:
Clin Image Based Proced. 2016 ; 2016: 60–67. doi:10.1007/978-3-319-46472-5_8.

Personalized Optimal Planning for the Surgical Correction of Metopic Craniosynostosis

Antonio R. Porras[1], **D. Zukic**[2], **A. Equobahrie**[2], **Gary F. Rogers**[3], and **Marius George Linguraru**[1,4]

[1] Sheikh Zayed Institute for Pediatric Surgical Innovation, Children's National Health System, Washington DC, USA

[2] Kitware Inc., Carrboro, NC, USA

[3] Division of Plastic and Reconstructive Surgery, Children's National Health System, Washington DC, USA

[4] School of Medicine and Health Sciences, George Washington

Abstract

We introduce a quantitative and automated method for personalized cranial shape remodeling via fronto-orbital advancement surgery. This paper builds on an objective method for automatic quantification of malformations caused by metopic craniosynostosis in children and presents a framework for personalized interventional planning. First, skull malformations are objectively quantified using a statistical atlas of normal cranial shapes. Then, we propose a method based on poly-rigid image registration that takes into account both the clinical protocol for fronto-orbital advancement and the physical constraints in the skull to plan the creation of the optimal post-surgical shape. Our automated surgical planning technique aims to minimize cranial malformations. The method was used to calculate the optimal shape for 11 infants with age 3.8±3.0 month old presenting metopic craniosynostosis and cranial malformations. The post-surgical cranial shape provided for each patient presented a significant average malformation reduction of 49% in the frontal cranial bones, and achieved shapes whose malformations were within healthy ranges. To our knowledge, this is the first work that presents an automatic framework for an objective and personalized surgical planning for craniosynostosis treatment.

Keywords

Craniosynostosis; interventional planning; image registration; fronto-orbital advancement

1 Introduction

Craniosynostosis is a condition affecting 1 of every 2100-2500 [1] live births in which one or more cranial sutures fuse prematurely. In many cases, this results in an abnormal growth pattern of the cranial bones and malformations. If untreated, craniosynostosis can cause increased intra-cranial pressure, impaired brain growth, visual problems and cognitive delay [2].

Depending on which cranial suture is prematurely fused, craniosynostosis can be classified as sagittal, coronal, lambdoid or metopic. Furthermore, sometimes craniosynostosis can involve more than one suture. The case of metopic craniosynostosis is particularly challenging to diagnose, since the metopic suture fuses early in healthy subjects and, therefore, suture fusion alone is not an indicator of pathology. Studying the degree of malformation is then essential to assess metopic craniosynostosis and to decide if surgical intervention is necessary.

Fronto-orbital advancement [3] is a widely used interventional approach to correct for metopic craniosynostosis. During this intervention, the surgeon removes the frontal cranial bones and advances them forward to create a “normal” head shape with sufficient space to allow for healthy brain growth, as shown in Fig 1. However, how to create a normal cranial shape remains a subjective surgical art.

There is a lack of objective methods to quantify cranial malformations in clinical practice, which makes diagnosis, the decision to go for a surgery, and the intervention planning very dependent on the surgeon’s expertise. Mendoza et al. [4] proposed a method to quantify malformations objectively from CT images using a statistical atlas. In our work, we focus on the specific case of metopic craniosynostosis, and we base on the method to quantify malformations from [4] to address the problem of creating the optimal post-surgical shape via fronto-orbital advancement surgery.

Some previous works have addressed the need of interventional planning for fronto-orbital advancement. However, most reported techniques are based on free-hand approaches for advancing the lateral supraorbital region [5, 6]. Other works [7, 8] proposed the use of a set of predefined templates and computer aided design software packages to plan fronto-orbital advancement interventions. However, none of these approaches solved the problem of objectively finding a personalized and optimal shape to target during the intervention, since they were based on subjective assessment of malformations. In addition, manual human interaction was necessary in all these works and the results were still very dependent on the specialist.

Our automated method employs image registration through a novel and invertible poly-rigid transformation inspired by [9]. Importantly, our technique incorporates the concept of purely rigid regions within the clinical protocol for fronto-orbital advancement surgery to create the optimal personalized cranial shape to target during cranial shape remodeling. In addition, it does not only provide the surgeon with a shape to target during the intervention, but it also calculates how much each bone has to be displaced during the intervention in mm. To our knowledge, this is the first time a fully automatic and objective method is proposed for fronto-orbital advancement planning.

2 Methods

2.1 Objective quantification of malformations

CT is the standard imaging modality used to assess cranial deformities. To quantify malformations, we used the approach described in [4]. To summarize, a patient’s cranium was registered to a reference image template. Once the volumes were aligned, a single-layered, genus-zero surface was obtained using ShrinkWrap [10], obtaining a triangular mesh representing the cranial shape as a result. Then a template-guided graph-cut method based on [11] was used to segment cranial bones and sutures from the volume segmented from the CT image. Note that with such an approach, in presence of a fused suture, the segmentation algorithm is only driven by the template and the suture is delineated as in the template. Finally, cranial malformations were quantified in relation to the closest normal shape extracted from a statistical atlas built from healthy subjects using Signed Distance Function (SDF) representations of the surfaces, thus avoiding the problems related to landmark correspondences.

2.2 Optimal personalized intervention planning

In this section, we introduce a method to plan the correction of metopic craniosynostosis via fronto-orbital advancement. Finding the optimal shape to target during the intervention can be viewed as an optimization problem, where a function quantifying the degree of malformations in the patient’s skull has to be minimized. We propose a solution based on image registration, where the goal is to deform the volumetric image of the subject's skull to minimize its malformations. In particular, we register the volumetric image of the subject's skull to the image of the closest normal skull in the statistical shape atlas. Our framework incorporates physical constraints, namely bone rigidity, and also constraints imposed by the clinical protocol of fronto-orbital advancement, namely that only the position of the frontal bones can be modified during surgery.

A simple solution could be to estimate a rigid transformation for each of the bones separately. Instead, we employ a global registration approach to include interactions between bones and avoid bone overlaps. In [12], a method to incorporate rigid regions to an image registration problem was proposed, while allowing other types of deformation in the rest of the image. A set of rigid transformations (one per rigid object) and a global deformable transformation were linearly combined, using distance functions applied to each object to estimate the weight of its transformation at any location in the image. Such scheme ensured the weight associated to the non-linear transformation to equal zero in the rigid regions. However, the method did not guarantee invertibility of the estimated transformation. In addition, the accuracy was limited by the refinement of the underlying grid of control points and the smoothness of the radial basis functions.

In [9], a method to estimate a global transformation by combining the speed vectors from a set of rigid transformations centered on fixed anchor points was proposed. Unlike most free-form deformation approaches, this type of poly-rigid transformations solved problems related to large movements of objects. In addition, the resulting transformation was invertible. However, although the transformation was calculated from a set of local rigid transformations, no single region in the image was constrained to present a purely rigid transformation, as required in our application.

In our work, we extend the method presented in [9] by incorporating the concept of rigid regions introduced in [12], instead of using anchor points to define rigid transformations. Unlike in [12], we avoid the constraints related to using radial basis functions to define the transformation and we propose to use smooth, continuous and differentiable weighting functions to control the transition between rigid and non-rigid regions, thus ensuring the invertibility of the transformation.

Transformation model—The speed vector at a point with coordinates $\boldsymbol{x}$ is calculated by averaging the speed vectors from each rigid transformation of an object [9]:

$$\nu(\boldsymbol{x}, s) = \frac{\sum_{\forall i} w_i(\boldsymbol{x})\, \nu_i(\boldsymbol{x}, s)}{\sum_{\forall i} w_i(\boldsymbol{x})}, \quad (1)$$

where $\nu_i(\boldsymbol{x},s)$ is the speed vector associated to the rigid transformation i at coordinates $\boldsymbol{x}$ and time $s \in [0,1]$, and $w_i(\boldsymbol{x})$ is the weight of that rigid transformation at location $\boldsymbol{x}$. The speed vector associated to each rigid transformation is calculated as:

$$\nu_i(\boldsymbol{x}, s) = \boldsymbol{t}_i + \boldsymbol{A}_i(\boldsymbol{x} - s\boldsymbol{t}_i), \quad (2)$$

where $\boldsymbol{t_i}$ is the translation vector of the rigid transformation i, and $\boldsymbol{A_i}$ is a skew matrix. Eq. (2) is obtained by differentiating the trajectory equation $\boldsymbol{T}(\boldsymbol{x},s) = s\boldsymbol{t_i} + exp(s\boldsymbol{A_i})\boldsymbol{T}(\boldsymbol{x},0)$. The matrix $\boldsymbol{A_i}$ is defined as the logarithm of the rotation matrix and is related to the rotation vector by the following equation [9]:

$$\boldsymbol{A}_i = \begin{pmatrix} 0 & -r_z & r_y \\ r_z & 0 & -r_x \\ -r_y & r_x & 0 \end{pmatrix}, \quad (3)$$

where $\boldsymbol{r} = (r_x, r_y, r_z)$ is the rotation vector. In [9], the weights $w_i(\boldsymbol{x})$ were calculated using Gaussian functions centered at each anchor point defined on the image. This approach does not allow constraining different areas of the image to be purely rigid. In addition, the weighting functions proposed in [12] would not ensure the invertibility of the transformation, since they are not differentiable at the boundary of the rigid objects.

In our implementation, the rotation of each transformation is defined to be centered on the center of mass of the rigid object associated to it. We also calculate SDFs for each of the rigid objects in the image (i.e. the cranial bones), which take negative values inside the object and positive values outside. The weight function associated with the transformation of each rigid object can then be defined using a continuous, smooth and differentiable approximation to a Heaviside step function applied to the SDF of that object:

$$w_i(\boldsymbol{x}) = \frac{1}{1 + \exp(c \quad SDF_i(\boldsymbol{x}))}, \quad (4)$$

where $SDF_i(\boldsymbol{x})$ is the SDF calculated for object i at coordinates $\boldsymbol{x}$, and c is a factor defining the slope of the function at the transition point (i.e. the object boundary).

Next, we integrate the velocity at each point over time to estimate the trajectory according to the transformation model. A second-order discretization scheme was proposed in [9] by defining the following operator:

$$\boldsymbol{T}^{1/N}(\boldsymbol{x},s) = \boldsymbol{x}+\frac{\sum_{\forall i} w_i(\boldsymbol{x})\left(\frac{1}{N}\boldsymbol{t}_i+(\exp(\boldsymbol{A}_i/N)-\boldsymbol{I})(\boldsymbol{x}-s\boldsymbol{t}_i)\right)}{\sum_{\forall i} w_i(\boldsymbol{x})}, \quad (5)$$

where $\boldsymbol{I}$ represents the identity matrix, and N is the number of discretization subintervals. Using Eq. 5, the trajectory of a point at coordinates $\boldsymbol{x}$ can be obtained recursively from the composition of that operator at different time instants: $\boldsymbol{T}(\boldsymbol{x}) = \boldsymbol{T}^{1/N}(.,(k-1)/N)\circ\ldots\circ\boldsymbol{T}^{1/N}(\boldsymbol{x},0)$. In our implementation, we divide the temporal interval empirically into two subintervals. Although this number of discretization intervals was enough for our goal, in applications where larger displacements can be expected, discontinuities may appear and a higher discretization level may be chosen.

Dissimilarity measure—Our application aims to minimize deformities in the subject's skull. In [4], the degree of malformation was quantified as the distance between the subject's cranial shape and the reference shape (i.e. closest normal subject). In the image domain, this translates to minimizing the pixel intensity difference between the volumetric image of the patient's cranium and the closest normal subject:

$$\boldsymbol{D}(F,M) = \sum_{\forall \boldsymbol{x}}(M(\boldsymbol{T}(\boldsymbol{x}))-F(\boldsymbol{x}))^2, \quad (6)$$

where M is the patient's image, and F is the closest normal subject's image.

Optimization—We used a regular gradient descent optimizer for the objective function. Given the transformation model described above, a set of parameters defining as many rigid transformations as objects (i.e. cranial bones) can be optimized. However, for the surgical treatment of metopic craniosynostosis via fronto-orbital advancement, only the cranial frontal bones require advancement, while the rest of the bones are kept in the same position during the intervention. For that reason, the optimization is constrained so the translation and rotation parameters of the non-frontal bones are not modified.

Evaluation—For each patient with metopic craniosynostosis, malformations were quantified using the method summarized in section 2.1. After segmenting the cranial bones and sutures as in [4], we used our method to register the binary volumetric images of the patient's skull to its closest normal from the statistical atlas. The estimated transformation calculated was then applied to the subject's cranial shape to obtain the optimal shape to target during the intervention. As an example, Fig. 2 shows the interventional plan calculated for one example patient with severe metopic craniosynostosis.

2.3 Data

To create the statistical atlas of normal cranial shapes, we used axial CT images of 100 healthy infants (age 5.80±3.31 months). In-plane pixel size ranged 0.26-0.49 mm, with axial spacing smaller or equal to 5mm, in line with common clinical practice for craniosynostosis [13]. For the experiments, we used retrospective CT images from 11 subjects (age 3.8±3.0 months) diagnosed with metopic craniosynostosis.

3 Results

Average malformations calculated for the 11 cases analyzed were 3.12±1.38 mm for the right frontal (RF) bone and 3.34±1.52 mm for the left frontal (LF) bone. A Student's t-test was used to check if these results were statistically different to the results reported in [4] for patients with metopic craniosynostosis (3.20±2.07 mm for the RF bone and 2.57±1.71 mm for the LF bone). Differences were not statistically significant, obtaining $p = 0.90$ and $p = 0.23$ for the RF and LF bones, respectively.

After creating the optimal post-surgical shape, malformations were significantly reduced to 1.62±0.99 mm for the RF bone and 1.67±0.99 mm for the LF bone ($p < 0.01$), representing an average reduction of 49%. These values were within the range reported in [4] for healthy subjects (1.11±0.63 mm for the RF bone and 1.13±0.50 mm for the LF bone), with $p = 0.15$ and $p = 0.11$ for the RF and LF bones, respectively. As an example, Fig. 2 shows the interventional plan for one severe patient, where it is possible to observe a significant reduction of malformations in the frontal bones of the optimal post-surgical shape (c) with respect to the pre-operative shape (a). Note that, after the surgery, cranial bones will resume their normal growth and this will also play an important role in developing a normal skull shape.

4 Conclusions

Our technique for fronto-orbital advancement surgical planning, based on a method for an objective quantification of malformations, constitutes the first fully automatic and objective framework for metopic craniosynostosis assessment and interventional planning. We introduced a method based on image registration that takes into account bone rigidity and clinical protocol constraints, and computes a smooth and invertible transformation to reconstruct the optimal cranial shape during the intervention. We demonstrated that the post-surgical shape reconstructed with our method and the surgical plan to achieve it can significantly reduce malformations in the frontal bones by 49%. In addition, malformations in the optimal shapes obtained were within healthy ranges. Importantly, we do not only provide the optimal shape to target during the intervention, but we also provide information about how much each bone has to be displaced and in which direction to achieve that optimal shape.

Future work includes the integration of our method in the clinical workflow for its validation. It will also be adapted to allow for bone exchange and bending, considering the mechanical properties of the bones. Finally, the versatility of this framework will allow extending it for treatment planning of other types of craniosynostosis.

Acknowledgements

This work was partly funded by the National Institutes of Health, Eunice Kennedy Shriver National Institute of Child Health and Human Development under grant NIH 1R41HD081712 and 2R42HD081712.

5 References

1. Lajeunie E, Le Merrer M, Bonaïti-Pellie C, Marchac D, Renier D. Genetic study of nonsyndromic coronal craniosynostosis. Am. J. Med. Genet. 1995; 55:500–504. [PubMed: 7762595]
2. Wood BC, Mendoza CS, Oh AK, Myers E, Safdar N, Linguraru MG, Rogers GF. What's in a Name? Accurately Diagnosing Metopic Craniosynostosis Using a Computational Approach. Plast. Reconstr. Surg. 2016; 137:205–213. [PubMed: 26710024]
3. Aryan HE, Jandial R, Ozgur BM, Hughes SA, Meltzer HS, Park MS, Levy ML. Surgical correction of metopic synostosis. Child's Nerv. Syst. 2005; 21:392–398. [PubMed: 15714353]
4. Mendoza CS, Safdar N, Okada K, Myers E, Rogers GF, Linguraru MG. Personalized assessment of craniosynostosis via statistical shape modeling. Med. Image Anal. 2014; 18:635–646. [PubMed: 24713202]
5. Havlik RJ, Azurin DJ, Bartlett SP, Whitaker LA. Analysis and treatment of severe trigonocephaly. Plast. Reconstr. Surg. 1999; 103:381–390. [PubMed: 9950522]
6. Selber J, Reid RR, Gershman B, Sonnad SS, Sutton LN, Whitaker LA, Bartlett SP. Evolution of Operative Techniques for the Treatment of Single-Suture Metopic Synostosis. Ann. Plast. Surg. 2007; 59
7. Burge J, Saber NR, Looi T, French B, Usmani Z, Anooshiravani N, Kim P, Forrest C, Phillips J. Application of CAD/CAM Prefabricated Age-Matched Templates in Cranio-Orbital Remodeling in Craniosynostosis. J. Craniofac. Surg. 2011; 22:1810–1813. [PubMed: 21959440]
8. Diluna ML, Steinbacher DM. Simulated Fronto-Orbital Advancement Achieves Reproducible Results in Metopic Synostosis. J. Craniofac. Surg. 2012; 23:231–234.
9. Arsigny V, Pennec X, Ayache N. Polyrigid and polyaffine transformations: A novel geometrical tool to deal with non-rigid deformations - Application to the registration of histological slices. Med. Image Anal. 2005; 9:507–523. [PubMed: 15948656]
10. Pope, P. Shrinkwrap : 3D Model Abstraction for Remote Sensing; 2009 ASPRS Annual Meeting; 2009. p. 9-13.
11. Liu, L., Raber, D., Nopachai, D., Commean, P., Sinacore, D., Prior, F., Pless, R., Ju, T. MICCAI. LNCS; 2008. Interactive separation of segmented bones in CT volumes using graph cut; p. 296-304.
12. Little, JA., Hill, DLG., Hawkes, DJ. Deformations incorporating rigid structures [medical imaging]; Workshop on Mathematical Methods in Biomedical Image Analysis; IEEE; 1996. p. 223-232.
13. Vannier MW, Pilgram TK, Marsh JL, Kraemer BB, Rayne SC, Gado MH, Moran CJ, Mcalister WH, Shackelford GD, Hardesty RA. Craniosynostosis: Diagnostic Imaging with Three-Dimensional CT Presentation. Am. J. Neuroradiol. 1994; 15:1861–1869. [PubMed: 7863936]

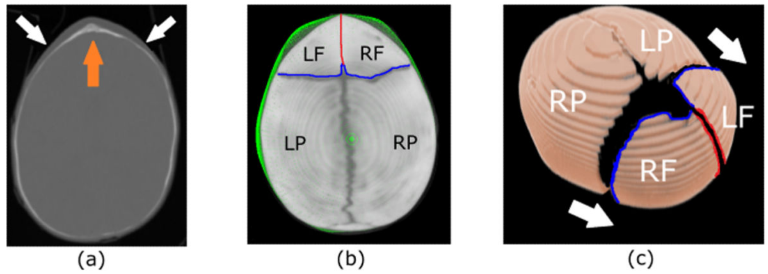

Fig. 1.

Metopic craniosynostosis and fronto-orbital advancement. (a) Axial plane view of the CT image on one patient with metopic craniosynostosis. White arrows show major areas with malformations. The orange arrow shows ridging on the fused metopic suture. (b) Cranial volume of the patient in (a) extracted from CT, together with its closest normal shape (green) estimated as in [4]. The coronal sutures are delineated in blue and the fused metopic suture is shown in red. (c) Representation of the personalized optimal shape to target during a frontoorbital advancement intervention, where the left (LF) and right frontal (RF) bones are advanced forward with respect to the left (LP) and right parietal (RP) bones.

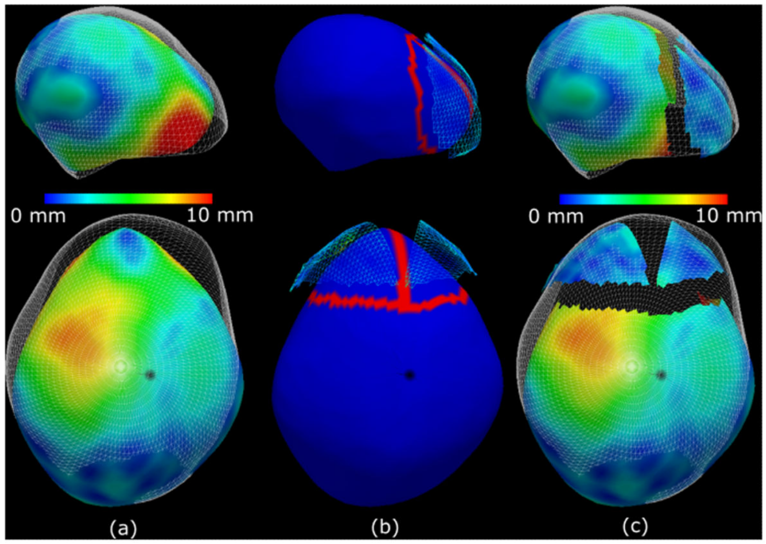

Fig. 2.

Surgical planning. (a) Lateral (top) and axial (bottom) views of the malformations (color coded) estimated on one patient's skull shape, together with its closest normal shape (white wireframe). (b) Suggested cut lines (red) based on coronal and metopic sutures segmentation, together with the optimal position for the frontal bones computed with the proposed method, shown as a wireframe. (c) Malformations estimated on the optimal post-surgical shape, together with its closest normal shape (white wireframe).